PACE OCI Lunar Calibration: Initial Results

Shihyan Lee[1,2], Frederick Patt[1,2], Robert E. Eplee[1,2], Jeffrey McIntire[1,3], and Gerhard Meister[1]

[1]NASA Code 616, Ocean Ecology Lab, Goddard Space Flight Center, Greenbelt, Greenbelt Rd., Maryland, MD 20771, USA
[2]Science Applications International Corporation, 12010 Sunset Hills Rd., Reston, VA 20190, USA
[3]Science Systems and Application International, 10210 Greenbelt Road, Suite 600
Lanham, Maryland 20706, USA

ABSTRACT

Launched in February 2024, the Ocean Color Instrument (OCI) onboard NASA's Plankton, Aerosol, Cloud, ocean Ecosystem (PACE) mission has started performing its monthly lunar calibrations at ±7 degrees lunar phase angle in March 2024. In this paper, we will describe the OCI lunar calibration methodology and show the results of lunar calibration events during the initial months of PACE/OCI operation. A key difference of OCI lunar calibration from heritage sensors is that the lunar disk integrated irradiance is computed from lunar pixel radiance and sampling distance instead of the instrument's IFOV. PACE provided a near constant sweep rate during lunar calibration allowing accurate determination of OCI pixel sampling extent. OCI performs lunar calibration in baseline science mode with 282 hyperspectral bands from 315 – 895 nm and 7 shortwave infrared bands (940 - 2260 nm). For each OCI band, we compute the integrated lunar disk irradiance, and compare the result with a lunar irradiance model (ROLO) prediction. The early results presented here clearly show that OCI's lunar image acquisition is working as intended and will provide accurate data for OCI's on-orbit radiometric characterization. The hyperspectral lunar irradiances provided by OCI are expected to become a valuable dataset for the evaluation of lunar irradiance models.

Keywords: PACE, OCI, moon, calibration.

1. INTRODUCTION

Launched in February 2024, NASA's Ocean Color Instrument onboard PACE mission becomes the first satellite sensor to provide moderate spatial resolution (1km), hyper-spectral resolution (1.25-5nm) from UV to Near Infrared Red (NIR) and 7 Short-Wave-Near-Infrared (SWIR) multi-spectral bands at daily global coverage [1]. This engineering challenge is achieved by two CCDs recording signals in a blue (315-610nm) spectrograph, a red (600-895 nm) spectrograph and a separate SWIR Detector Assembly (SDA) [2]. On-orbit, routine solar and lunar calibrations are performed as the two main calibration activities to track OCI's radiometric performance. The solar calibration is the primary approach to trend the short and long term OCI detector gain change and to track potential change in linearity [3]. The lunar calibration will be used to verify the long-term stability of solar calibration and make adjustment to long term OCI detector gain trends if necessary.

To achieve the stringent requirement of the ocean climatology dataset [4, 5], lunar calibration is a commonly used method to achieve the long-term radiometric calibration stability [6–8]. The Moon is an ideal calibration target as its surface is photometrically stable [10] and it can be observed without atmospheric contamination. The geometrically corrected apparent lunar reflectance can be obtained from the US Geological Survey's Robotic Lunar Observatory (ROLO) photometric model [11] using the observation time and the satellite position, which determines the lunar phase and libration angles, as well as Sun–Moon and satellite–Moon distances. The lunar irradiance can be estimated as the product of solar irradiance model and ROLO predicted apparent lunar reflectance after adjusting for the Sun–Moon and satellite–Moon distances. The OCI detector gain can be determined by the ratio from the model predicted and OCI measured lunar irradiances.

2. OCI LUNAR OBSERVATION

The OCI lunar calibration is performed at 2 targeted lunar phase angles, ±7 degrees. In addition to the ±7 degrees phase angles, we have performed lunar calibrations at other phase angles (e.g., -55 and -51 degrees) to be able to compare the results to other sensors. Within each lunar calibration event, the moon is observed twice via a forward and a backward lunar pass (Figure 1a). A series of PACE spacecraft maneuvers were performed to precisely control the lunar sweep rate and the lunar observation scan angle within OCI's field of regard. The targeted lunar sweep rate is 0.125 degree/sec, which is about 4 times slower than the sweep rate during the normal science operation. This allows the moon to be over-sampled 4 times. The targeted lunar view angle is at 30 degrees. For all early mission lunar calibrations, the actual OCI sweep rates and lunar view angles show minimum deviation from the targeted values.

In Figure 1a, the arrows indicate the OCI's lunar ground tracks of the forward and backward observations. Figure 1b shows the lunar sweep rate along the OCI's lunar ground tracks, calculated using spacecraft attitude information. The OCI lunar sweep rate is computed at the scan angle at the center of the moon. In Figure 1b, since the moon is only observed for the red portion of the curve, the rest (in black) can be regarded as pseudo lunar sweep rate (computed at the same scan angle as the view angle of the moon) as the moon wasn't within OCI's field of view.

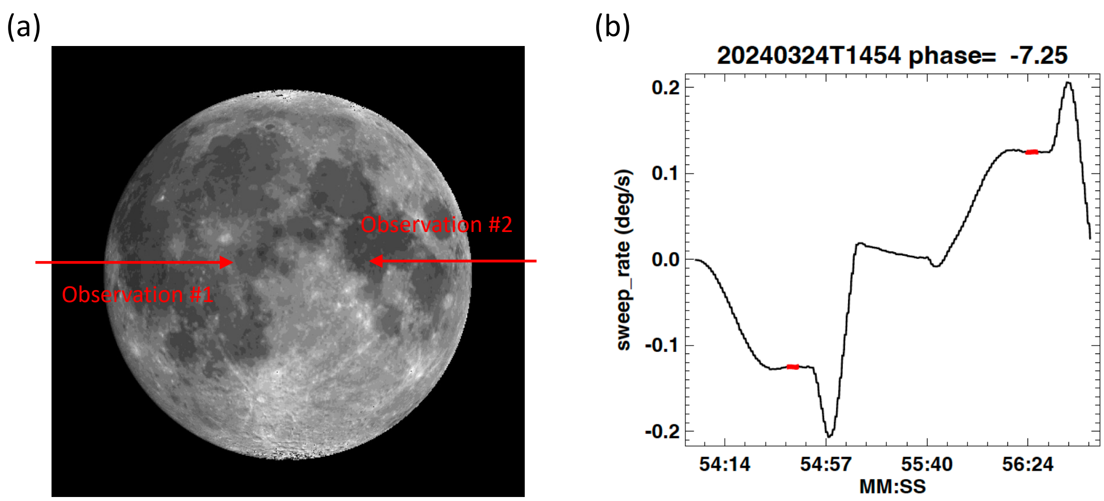

Figure 1. OCI lunar calibration. (a) The OCI makes 2 passes (one sweep in forward and one in backward direction) during each lunar calibration event through a series of spacecraft maneuvers. (b) OCI sweep rate during lunar calibration. The 2 lunar observations are highlighted in red.

Figure 2 shows the lunar images from the first OCI lunar calibration performed at -7 degree phase angle on March 24, 2024. All bands on the red focal plane were averaged to create an image with higher SNR. Figure 2 shows the images in forward (2a) and backward (2b) passes are mirrored along the vertical axis. The comparison of Figure 1a and Figure 2 shows that the reversed ground track direction is the result of reversed spin number in the lunar images. The lunar image is not mirrored along the pixel (horizontal) direction as the OCI scan direction is the same between forward and backward observations.

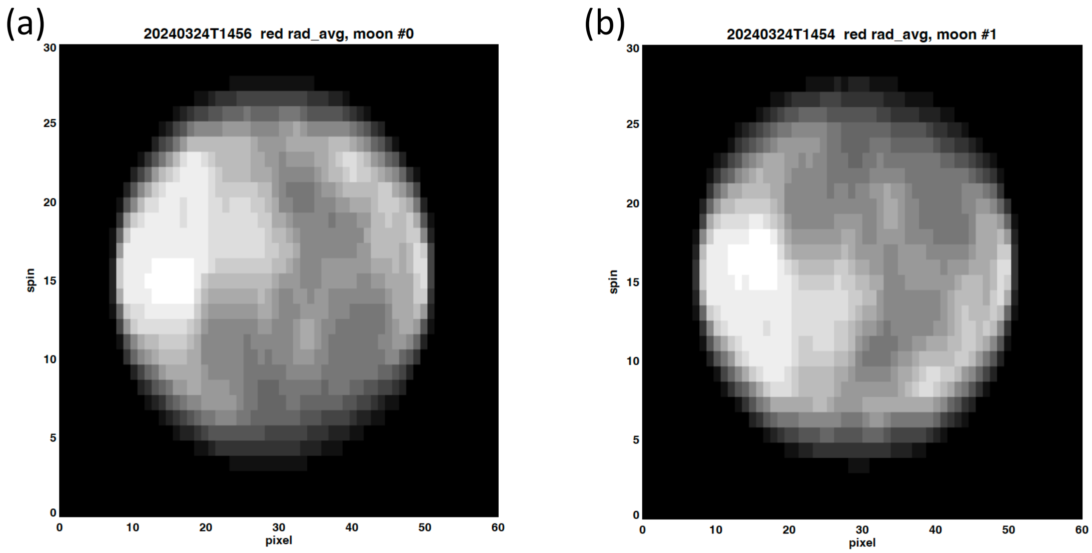

Figure 2. OCI red bands averaged lunar images for (a) forward observation and (b) backward observation. Notice the reverse brightness pattern between forward and backward observation.

Figure 3 shows the OCI sweep rate around the lunar observations. It shows the sweep rate is extremely stable during the lunar observations (in red). Within each lunar observation, the standard deviation of the sweep rates is 0.2% or less and there is no measurable drift. The sweep rates between the two lunar observations are differed by only about 0.4%. The near constant lunar sweep rates indicate a near constant over-sampling rate. This will in turn remove lunar observation uncertainty due to over-sampling rate variations [12].

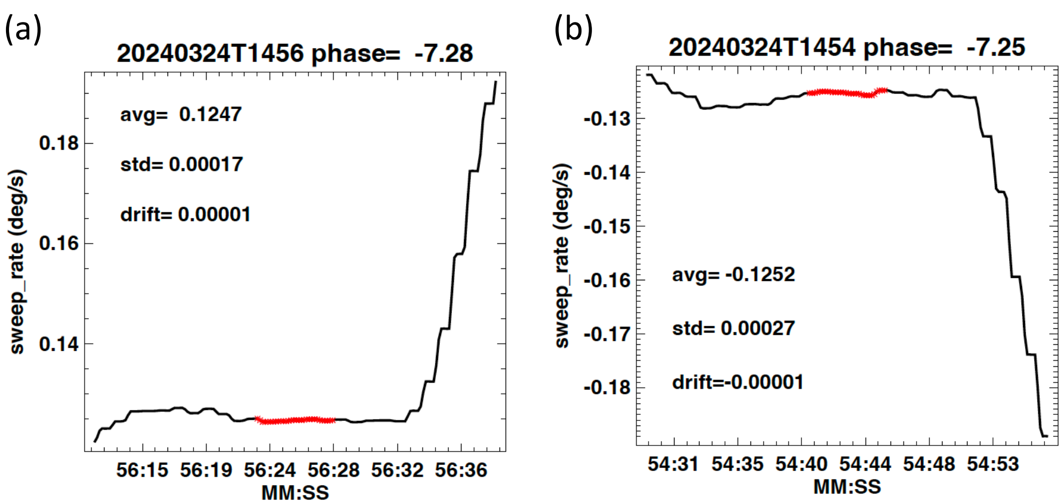

Figure 3. OCI sweep rate during lunar observations at (a) forward and (b) backward directions. The lunar observations are highlighted in red. The mean, standard deviation and drift during the lunar observation are shown in the plot.

3. OCI LUNAR CALIBRATION

In the OCI lunar calibration, the main objective is to determine the lunar gain, which is computed as the ratio of the OCI observed lunar irradiance and the model estimated lunar irradiance. Based on lunar gain, we can assess OCI calibration performance in OCI detector gain trending, detector ham side ratio, response versus scan angle (RVS) and detector gains' relative spectral accuracy and make calibration adjustment if necessary.

To compute the model estimated lunar irradiance, we first spectrally interpolate the ROLO estimated apparent lunar reflectance between the ROLO bands to cover the OCI bands. In Figure 4a, the symbols indicate the ROLO model output reflectance at ROLO bands and the red curve is the interpolated values at 0.1 nm interval. The 0.1 nm step was chosen to match the resolution of the Total and Spectral Solar Irradiance Sensor (TSIS) model [13], used in OCI data processing. Using the interpolated apparent lunar reflectance, we can compute the model estimated lunar irradiance in the fine 0.1nm spectral resolution, after adjusting for sun-moon and spacecraft-moon distances. Finally, the model predicted lunar irradiance at each OCI band is computed by integrating the lunar spectral irradiance with the Relative Spectral Response (RSR) of the OCI bands. In Figure 4b, the red lines are the model predicted lunar spectral irradiance at 0.1nm spectral sampling and the black symbols are the predicted integrated lunar irradiances at each OCI band.

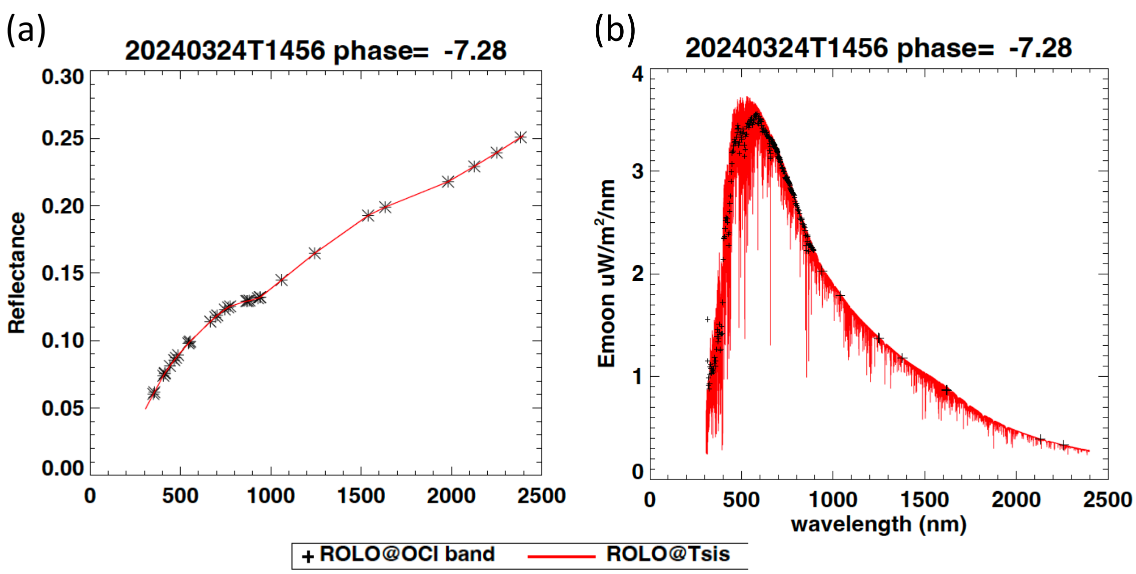

Figure 4: (a) ROLO model output reflectance at 32 wavelengths (symbol), interpolated into 0.1 nm steps (red curve). (b) Lunar irradiance model (Emoon) estimated from interpolated ROLO lunar reflectance and TSIS solar irradiance model (red); and model estimated lunar irradiance at each OCI band (black symbols).

The OCI measured lunar irradiance is computed as the sum of each measured lunar pixel radiance multiplied by the pixel sampled area (A) determined by Ground Sampling Distance (GSD).

$$E_{oci}(b) = \sum_{i=0}^{n} L_i(b) * A(b) \quad \text{eq. 1}$$

$$A(b) = GSDx(b) * GSDy(b) \quad \text{eq. 2}$$

In eq. 1, $E_{oci}(b)$ is the OCI lunar irradiance at band b, $L_i(b)$ is the measured band b radiance at pixel i, and $A(b)$ is the pixel sampling area of band b. $L_i(b)$ were calculated with a provisional OCI gain calibration (used in PACE reprocessing V2, see https://oceancolor.gsfc.nasa.gov/data/reprocessing/V2.0/pace/) without temporal correction (K2 = 1). The pixel sampling area is defined as the product of ground sampling distance at scan (GSDx) and track directions (GSDy) (eq. 2). The prelaunch measured GSDx is used as it is accurately determined [14], and the GSDy can be computed from the OCI's lunar sweep rate.

Note that previously, measured lunar irradiance was typically calculated by replacing A(b) in equation 1 by the instantaneous field of view (IFOV) of an image pixel. The approach chosen here was derived after a discussion at the Fourth Joint GSICS/IVOS Lunar Calibration Workshop in Darmstadt, Germany, December 2023, and an email from Hugh Kieffer (personal communication). The recommendations from the workshop have not been finalized yet, the approach chosen here is our understanding of the optimal implementation for the OCI instrument, and it has not been peer reviewed. However, we believe pixel sample area can be more precisely determined by GSD than the IFOV. This method can also be applied to other sensors such as SeaWiFS, MODIS, and VIIRS to improve the overall lunar calibration accuracy.

The OCI sweep rate during lunar calibration is ~0.125 degrees/sec (Figure 3). The OCI telescope spin rate of 5.699 Hz, corresponding to a sweep rate of ~0.022 degrees/spin (GSDy = 0.022 degree). Compared to the nominal OCI GSD of ~0.088 degree, the lunar calibration sweep rate is about 4x slower than the sweep rate during normal science data collection. The 4x slower sweep rate results in an oversampling rate of 4. The 4x oversampling rate is our operational target, and it has been maintained throughout the early months of lunar calibration events.

In Figure 2, the -7 degree lunar image is roughly a circle. This is achieved by scaling the pixel number along scan and track (spin) direction to match their corresponding GSDs. During lunar calibration, the OCI is configured to be sampled at its physical pixel resolution, or 1/8 science pixel (see [2] for an explanation of different OCI aggregation modes) in the along scan direction. 1/8 science pixel corresponds to ~0.011 degree, which is about 2x smaller than the 0.022 degree in along track GSD from successive spins. Therefore, the 60x30 pixel image in Figure 2 displays the moon in an approximately correct aspect ratio.

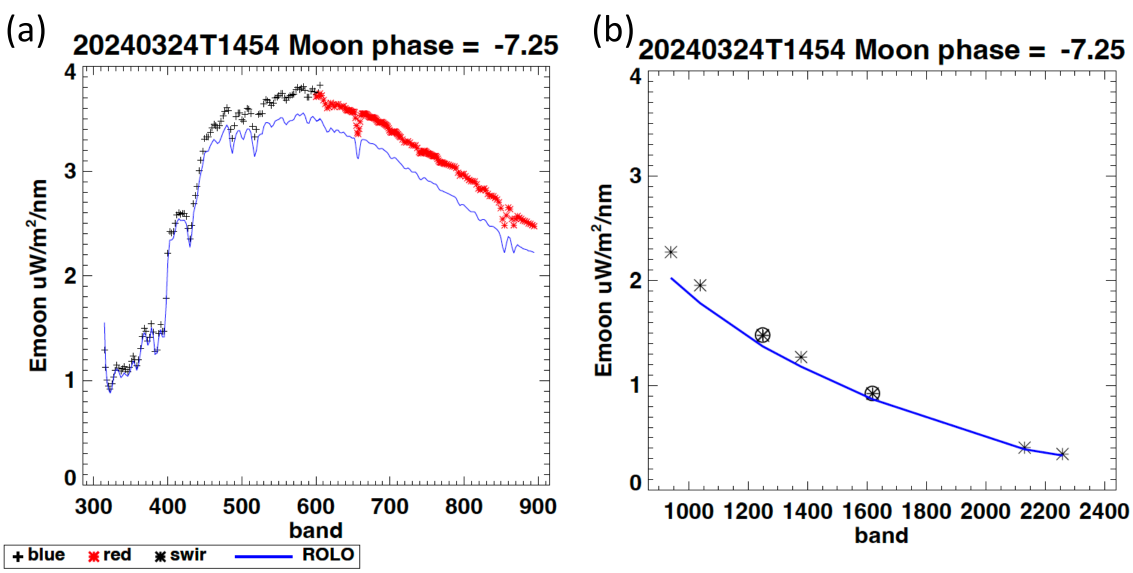

Figure 5: OCI measured vs. ROLO model predicted lunar irradiance. (a) blue and red FPA hyperspectral bands (b) SWIR bands; circles are the high gain bands.

Figure 5 shows the OCI measured lunar irradiance overplotted with model prediction for the hyperspectral bands (Figure 5a) and the SWIR bands (Figure 5b). The OCI and model predicted lunar irradiance have similar spectral shapes although the OCI measured lunar irradiance is higher overall. Figure 6 shows the lunar gain, the ratio of OCI measured and model predicted lunar irradiances. The lunar gain ratios show a clear spectral dependence with variations of up to 10%.

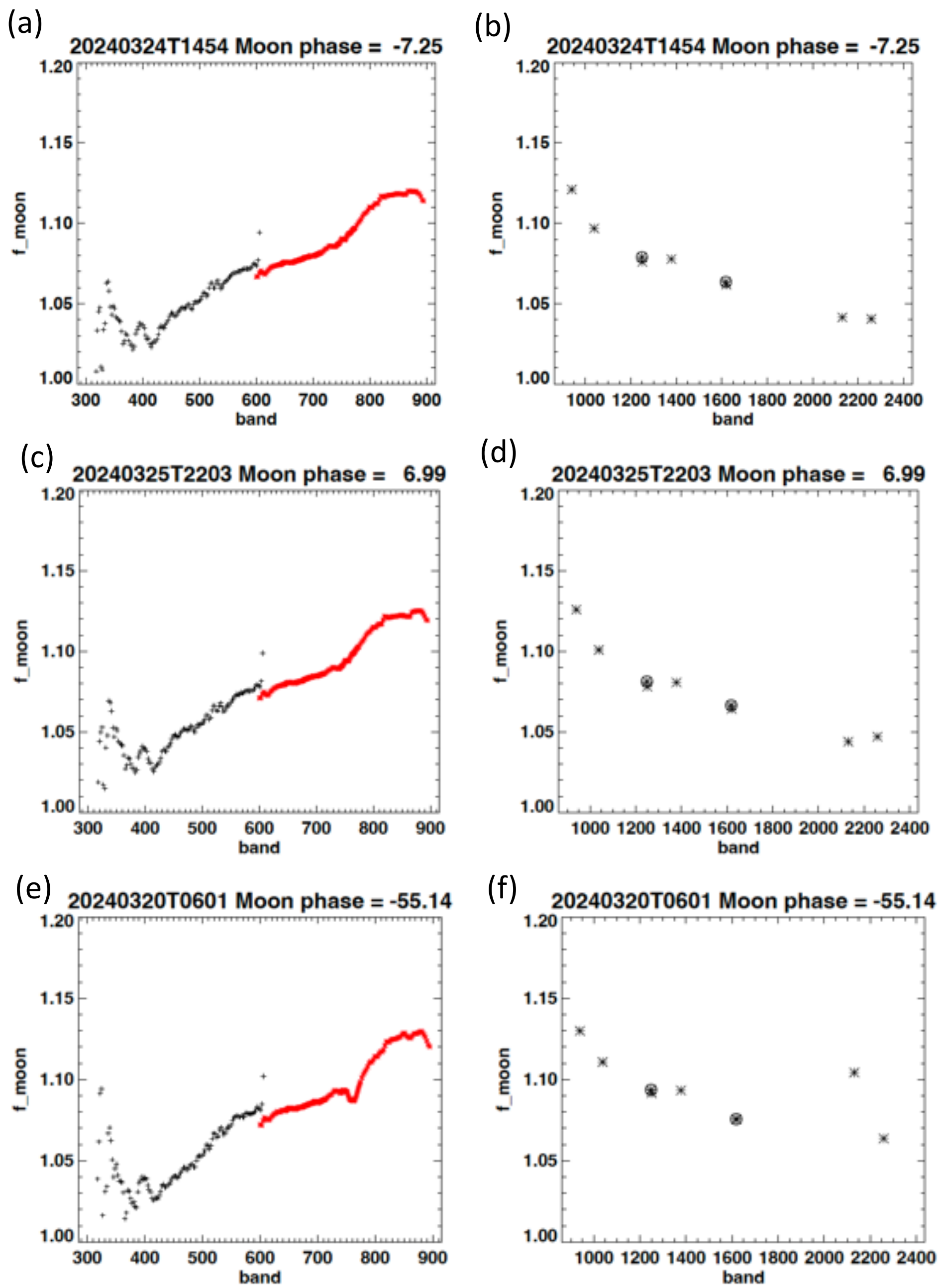

Figure 6: Ratio of OCI measured vs. ROLO model predicted lunar irradiance (f_moon = Emoon_oci/Emoon_model). (a, c, e) show blue and red FPA hyperspectral bands, (b, d, f) show SWIR bands; circles are the high gain bands. The targeted lunar phase angles are (a, b) -7 degree, (c, d) 7 degree, and (e, f) -55 degree.

4. EARLY RESULTS

In this paper, we will present results from the first 4 lunar calibrations at each of the designated phase angles, ±7 degrees. Figures 7 and 8 show the OCI lunar gain trending (K2_moon; see the OCI calibration equation in so for a definition of K2) for the -7 and +7 degree phase angle lunar data. K2_moon is computed as OCI lunar gain (f_moon) normalized to the first measurement. In the OCI calibration equation, K2 defines the normalized detector gain trends and is derived from solar calibration. Similarly, K2_moon defines the normalized detector gain trends but is derived from lunar calibration. K2_moon shows the different trends between -7 and +7 degree data are up to a few tenth of a percent. Since the OCI solar calibration results indicate little detector gain change at this point in the mission [4], these lunar gain variations are likely within the uncertainties in the OCI lunar calibration [15].

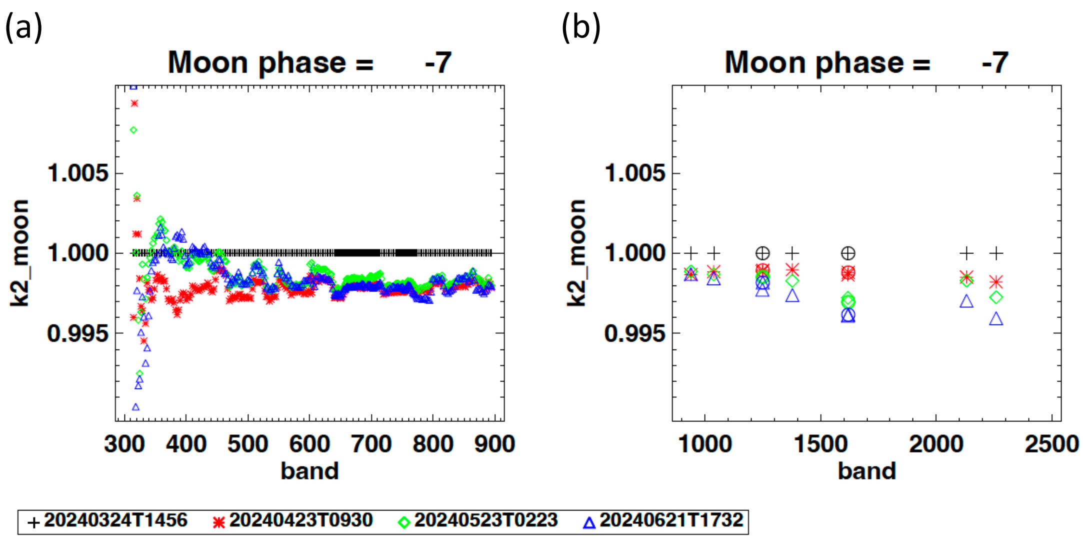

Figure 7: Normalized OCI lunar gain (K2_moon), K2_moon is computed as the f_moon normalized to the first measurement. The results of first 4 lunar calibration events at -7 degree phase angle are shown in (a) blue and red FPA hyperspectral bands (b) SWIR bands. Symbols indicate lunar calibration events with timing indicated in the legend.

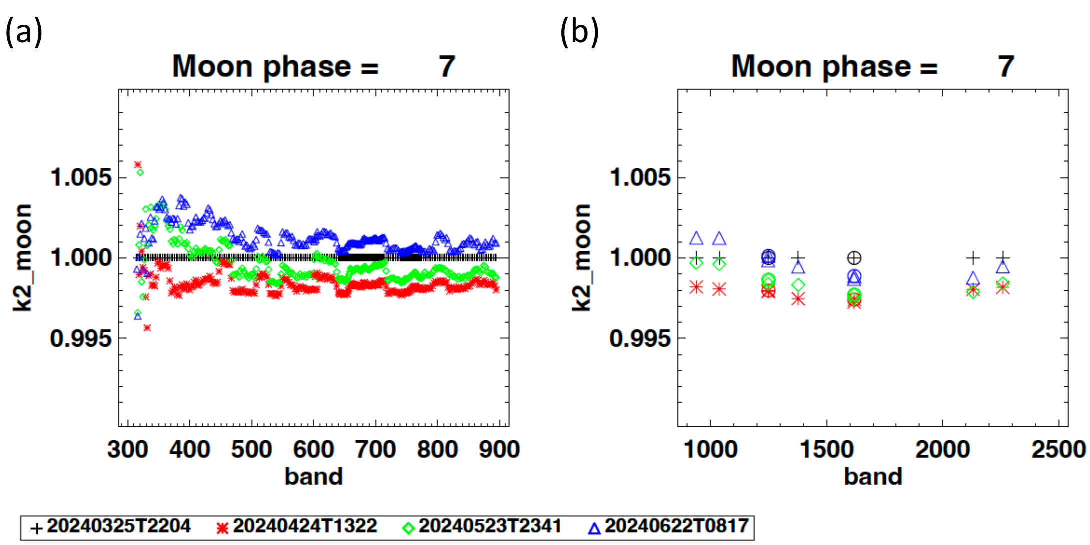

Figure 8: Normalized OCI lunar gain (K2_moon), K2_moon is computed as the f_moon normalized to the first measurement. The results of first 4 lunar calibration events at 7 degree phase angle are shown in (a) blue and red FPA hyperspectral bands (b) SWIR bands. Symbols indicate lunar calibration events with timing indicated in the legend.

One source of the uncertainty in OCI measured lunar irradiances is the accuracy of the lunar sweep rates. The lunar sweep rate determines a pixel's sampling area along the track direction, which directly impact the OCI measured lunar irradiance.

During each OCI lunar calibration event, two lunar observations were made. The forward and backward lunar observations are ~80 seconds apart, so we expect very good agreement in lunar calibration results. Figure 9 shows the ratio of lunar gain between forward and backward observations for each calibration events. There are clear biases between the forward and backward observation in some calibration events in the hyperspectral bands (Figure 9a) above 350 nm. The biases are most likely caused by the uncertainty in lunar sweep rate determination. The computed lunar sweep rate has an uncertainty of ~0.2% (Figure 3), which is likely the main cause of the forward/backward observation biases shown in Figure 9. The clear biases indicate the high noise-to-signal-ratio (SNR) of the lunar observations for hyperspectral bands above 350 nm. The SWIR band data are slightly nosier due to its lower spatial resolution. The data below 350 nm are noisy due to low SNR.

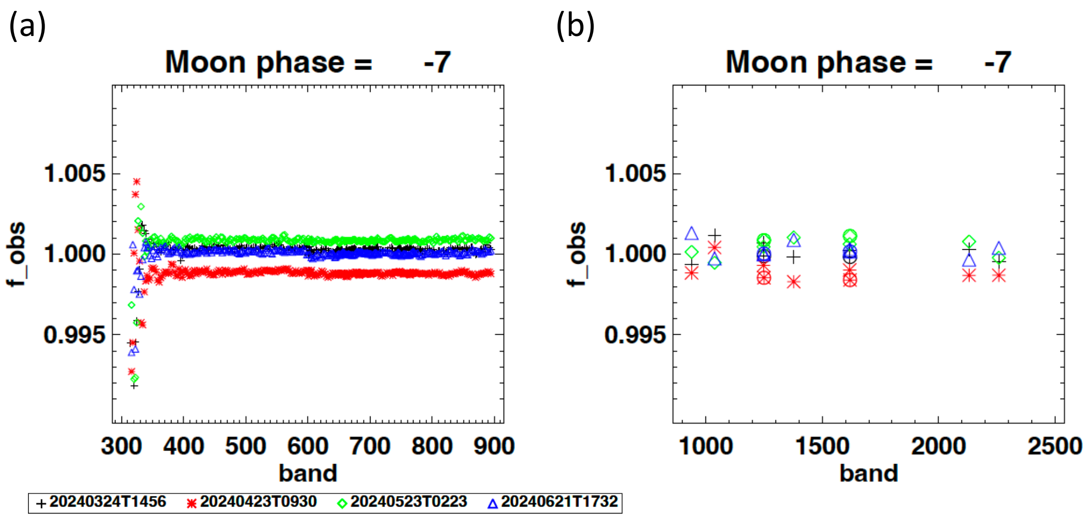

Figure 9: OCI lunar gain ratio between forward and backward observations (f_obs). The results of first 4 lunar calibration events at -7 degree phase angle are shown in (a) blue and red FPA hyperspectral bands (b) SWIR bands. Symbols indicate lunar calibration events with timing indicated in the plot legend.

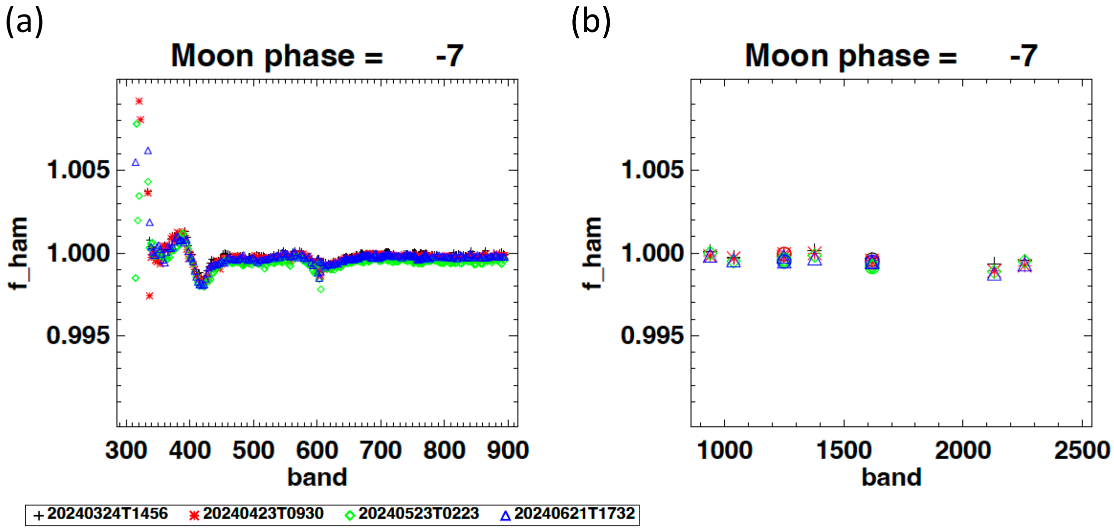

Figure 10: OCI measured lunar irradiance ham side ratio (f_ham). The results of first 4 lunar calibration events at -7 degree phase angle are shown in (a) blue and red FPA hyperspectral bands (b) SWIR bands.

The OCI uses a two-sided half angle mirror (HAM) to achieve wide view swath [2]. In every successive spin of the telescope, the alternating side of the HAM is used. As mentioned earlier, the OCI over-sampled the noon by 4 times, equivalent to a 2x oversampling for each HAM side. Figure 10 shows the ratio of OCI measured lunar irradiance between 2 HAM sides. For hyperspectral bands (Figure 10a), the HAM side ratios are around 1 except for the dichroic transition bands (~600 nm), and bands below 450 nm. Some SWIR bands also have the HAM ratio slightly deviate from unity (Figure 10b).

The most likely cause of the HAM side difference in OCI measured lunar irradiance is the residual of response-versus-scan (RVS) correction [2]. The OCI's nominal gain is computed at solar diffusor (SD) angle, which is at a different angle of incident (AOI) on the HAM than where the moon is observed. The biases in Figure 10 are most likely caused by residual error after RVS correction. Except for the UV bands, the HAM side biases in lunar irradiance are near constant over time without notable variation among lunar calibration events. The results indicate the lunar dataset has high enough SNR to detect changes as small as 0.1 percent. The measured lunar irradiance HAM ratio could become useful for tracking long-term OCI RVS stability.

5. CONCLUSION AND DISCUSSION

In this paper, we described the OCI lunar calibration methodology and presented the results from early mission OCI lunar calibration events. For each lunar calibration event, the lunar gain is computed as the ratio of OCI observed and model predicted lunar irradiance. The early mission lunar gains are used to evaluate the overall OCI calibration accuracy.

The OCI measured lunar irradiances are computed as the sum of the lunar pixel radiance multiplied by each pixel's sampling area. The sampling area of a pixel is defined as the ground sampling distances in both scan and track direction. In OCI, the ground sampling distances in scan direction is known precisely and the ground sampling distance of the track direction are computed from spacecraft attitude information. Compared to using the IFOV, which has commonly been used to calculate irradiance from image pixel radiances [6 – 9], the GSD method should be a more precise method to convert measured lunar pixel radiances to integrated lunar irradiance.

To properly capture the spectral features of the moon, the OCI lunar calibration uses the ROLO predicted apparent lunar reflectance and TSIS solar spectrum to produce a high spectral resolution, modeled lunar irradiance. Each OCI band's modeled lunar irradiance can be computed by integrating the high spectral resolution modeled lunar irradiance model with each OCI band's RSR.

The results from early mission lunar calibration events show the OCI measured lunar irradiance is about 2 – 12 % higher than the model predicted values. The measured-modeled lunar irradiance difference is highest in near-infrared bands and gradually decrease toward lower and higher wavelengths. Previous studies had shown ROLO modeled lunar irradiances are consistently lower than satellite observations [8,9]. However, the spectral dependency of the measured-modeled lunar irradiance varies among sensors, i.e. SeaWIFS, MODIS, and VIIRS, and is also different than what we saw in OCI. The root cause of this spectral dependency is currently under investigation. We believe our results are more reliable below 900nm than in the SWIR, because for the hyperspectral bands the calibration coefficients of the prelaunch GLAMR calibration (see [2]) agree within about 2% with the calibration coefficients derived from on-orbit solar diffuser measurements.

The early mission lunar gain trending did not show clear detector degradation. The early mission lunar gain variations were likely within the calibration uncertainties. In OCI measured lunar irradiance, the uncertainty in lunar sweep rate determination alone is ~0.2%. There is additional uncertainty from the model predictions. This result is consistent with OCI solar calibration where minimal detector gain changes were detected since the first lunar calibration event.

Just like in any new mission, the OCI lunar calibration methodology is constantly evolving. The Ocean Biological Processing Group (OBPG) calibration team will continue to improve lunar calibration, report any new findings and update lunar calibration results periodically.

REFERENCE:

[1] W., P. J., M. J. Behrenfeld, P. S. Bontempi, et al. 2019. "The Plankton, Aerosol, Cloud, ocean Ecosystem (PACE) mission: Status, science, advances." Bulletin of the American Meteorological Society, 100 (9): 1775–1794, 2019.

[2] G. Meister, Joseph J. Knuble, Ulrik Gliese, R. Bousquet, L. H. Chemerys, H. Choi, R. E. Eplee, R. H. Estep, Jr., E. T. Gorman, S. Kitchen-McKinley, D. Kubalak, S. Lee, C. McClain, J. W. McIntire, F. S. Patt, Z. Rhodes, P. Jeremy Werdell, "The Ocean Color Instrument (OCI) on the Plankton, Aerosol, Cloud, ocean Ecosystem (PACE) Mission: System Design and Prelaunch Radiometric Performance," in IEEE Transactions on Geoscience and Remote Sensing, doi: 10.1109/TGRS.2024.3383812.

[3] J. McIntire, S. Lee, R. E. Eplee, and G. Meister "PACE OCI On-orbit Solar Calibration". Proc. SPIE, Sensors, Systems, 13143-24, 2024, submitted.

[4] B. A. Franz et al., "Quality and consistency of the NASA ocean color data record," in Proc. Ocean Opt. XXI, Glasgow, Scotland (2012).

[5] National Research Council, "Climate data records from environmental satellites: interim report," The National Academies (2004).

[6] R. E. Eplee, Jr. et al., "On-orbit calibration of SeaWiFS," Appl. Opt. 51(36), 8702–8729 (2012).

[7] J. Sun et al., "MODIS reflective solar bands on-orbit lunar calibration," IEEE Trans. Geosci. Remote Sens. 45(7), 2383–2393 (2007).

[8] R. E. Eplee, Jr. et al., "A synthesis of VIIRS solar and lunar calibrations," Proc. SPIE 8866, 88661L (2013).

[9] J. Sun, R. E. Eplee, X. Xiong, T. Stone, G. Meister, and C. McClain, "MODIS and SeaWIFS On-Orbit Lunar Calibration," Proc. SPIE 7081, 70810Y (2008).

[10] H. H. Kieffer, "Photometric stability of the lunar surface," Icarus 130, 323–327 (1997).

[11] H. H. Kieffer and T. C. Stone, "The spectral irradiance of the Moon," Astron. J. 129, 2887–2901 (2005).

[12] S. Lee, G. Meister, F. Patt, and R. Eplee, "Estimating residual uncertainties for lunar irradiance measurements due to imaging acquisition parameters, " J. Appl. Remote Sens. 13(1), 014508 (2019), doi: 10.1117/1.JRS.13.014508.

[13] C., O. M., Richard, E. C., Harber, D., Pilewskie, P., Woods, T. N., Snow, M., et al. (2023). Version 2 of the TSIS-1 Hybrid Solar Reference Spectrum and Extension to the Full Spectrum. Earth and Space Science, 10, e2022EA002637. https://doi.org/10.1029/2022EA002637

[14] H. Choi, J. McIntire, S. Kitchen-McKinley, G. Meister, L. Chemerys, S. Lee, "Spatial characterization of PACE OCI ETU using time-delay mode," Proc. SPIE 12232, Earth Observing Systems XXVII, 1223211 (30 September 2022); https://doi.org/10.1117/12.2632640
[15] I. Cetinić, C. R. McClain, and P. J. Werdell, "PACE Technical Report Series, Volume 7", NASA/TM-2018-219027. https://pace.oceansciences.org/docs/TM2018219027Vol.7.pdf